Headquarters Papers
#UOET Proceedings 2023
https://www.milak.at/nike/uoet

doi: 10.5281/zenodo.10762118

Multi-Sensor Visibility Study based on a Hot Smoke Experiment in a Tunnel

Richard LADSTAEDTER (JOANNEUM RESEARCH)*

Stephan SCHRAML (AIT Austrian Institute of Technology)

Nikolaus STUDNICKA (RIEGL Laser Measurement Systems)

Emergency situations in tunnels require rescue teams supported by unmanned ground vehicels (UGV) to operate also in smoked tunnel areas. Such UGVs are equipped with various sensors (e.g. cameras, LiDAR or RADAR) to be able to navigate and quickly provide a common operational picture. Within the research project ROBO-MOLE experiments have been performed at the Zentrum am Berg at the Styrian Erzberg to directly compare the visibility range of RGB and thermal camera, LiDAR and RADAR in a hot smoke scenario.

Key Words: Visibility, tunnel, sensors, hot smoke

1. Introduction

Accidents in tunnels with impaired visibility are particularly dangerous, as they can often lead to personal injury. Most of the time, these visibility obstructions are related to a strong smoke development during fires. This is the motivation for the authors to test different sensors that are potentially capable of detecting people and other objects, e.g. vehicles, in a tunnel filled with hot smoke.

Therefore, the aim of this work is to comparatively investigate the impact of smoke in a road tunnel on the measurement range of different sensor technologies: RGB video camera, thermal camera, laser scanner (LiDAR, Light Detection And Ranging) and RADAR (Radio Detection And Ranging). In a suitable test, it should be checked under controlled conditions how the respective range is reduced by smoke, in particular at which density of the smoke no more meaningful measurement is possible. Visual observation by means of an RGB video camera serves as a standard of comparison.

The measurement of visibility conditions in a tunnel is very complex. A good introduction to the subject is given, for example, in the white paper of the SICK AG (Kuhn, 2018), which manufactures measuring devices such as the VISIC100SF installed in one of the ZAB tunnels. The focus there, however, was on the indirect determination of the pollutant load (dust) by measuring the transmission or scattering of light by the particles in the air. The (wavelength-dependent) absorption coefficient k describes approximately linearly the pollutant load along a path in an absorbing medium. However, since the real visibility depends, among other things, on the illuminance in the tunnel, there is only an indirect relation between the k-factor and the visibility.

(Pfennigbauer et al., 2014) and (Wallace et al., 2020) investigated the results of the online waveform processing of a comparable laser scanner in turbid media and in unfavorable weather conditions and its limitations. This investigation is complemented by the analysis of experimental results for measurements in a cloud chamber. It should be noted that a (moist) fog and a (dry and hot) smoke represent media with very different properties for a laser scanner operating with infrared light. However, the multi-target capability of the pulse-time-of-flight scanner used in this work is advantageous for both cases.

Existing studies in the field of robotics mainly use cold smoke to demonstrate e.g. the value of sensor fusion (e.g. LiDAR and RADAR) for navigation in difficult environments (cmp. Fritsche et al. (2016) and Mielle

*(corresponding author) Steyrergasse 17, 8010 Graz, Austria, richard.ladstaedter@joanneum.at

et al. (2019)). However, preliminary tests have clearly shown that cold smoke cannot reproduce a real fire situation. On the one hand, it is not the same medium, and on the other, the dynamics of smoke propagation are quite different (rise of hot gases, inhomogeneous distribution in the tunnel, etc.). For that reason, we only focus on hot smoke in this study.

The "Zentrum am Berg" (ZAB[1]) test tunnel in Erzberg, Austria, allows a realistic simulation of fire in a tunnel. On November 15, 2021 the underlying hot smoke tests for this work have been carried out there near the south portal in the so called „western railroad tunnel" within the research project ROBO-MOLE[2]. The tests have been under supervision of the professional fire department of Graz and Linz, respectively and have been performed in compliance with all necessary safety measures (suitable footwear, helmet, protective goggles).

The results and findings from our work may contribute to future improvements on sensor equipment and measurement techniques for autonomous robots when fighting fires in tunnels.

2. Sensors

The following sensors have been used in the hot smoke experiment and are listed with increasing wavelength:

- RGB video camera (visible light, 380-780nm, passive)
- Terrestrial laser scanner (infrared, 1.5µm, active)
- Thermal camera (LWIR, 8-14µm, passive)
- FMCW (Frequency-modulated continuous-wave) radar sensor (77GHz, W-band, 4mm, active)

Thus, these sensors (see Figure 1) used in the smoke test have very different modes of operation (active, passive), frequency ranges, and measurement principles. The radiation used by active sensors (LiDAR, RADAR) has to pass the smoky path twice, while it passes only once for passive sensors (visible light, LWIR).

For the latter, the distance of (non-self-illuminating) objects to the illumination source must also be taken into account. Thus, each sensor has individual strengths and weaknesses and is affected differently by smoke, which should be quantified by the present simultaneous measurements. The specifications or operating principle of each sensor are described in more detail below. Please note that each of those sensors just represents a whole class of sensors operating with the same measurement principle and in a similar frequency range. On the other hand, these specific sensors have been selected based on the requirements of the research project ROBO-MOLE. For example, the laser scanner, due to its advanced technology and processing techniques (waveform digitalization, multi echo detection) is considered specially suited for smoky environments and might outperform "standard" laser scanner models.

Figure 1: Sample illustrations of the sensors used (from left to right); RGB camera, thermal camera, laser scanner and FMCW RADAR.

[1] https://www.tunnellinghub.at/; https://www.zab.at/en [26/04/2023]

[2] Research project funded by the Austrian security research program KIRAS, project number: 879693.

a. RGB Camera

A VIVOTEK IB9381-HT V-series network camera has been used (see Table 1).

Table 1: RGB camera specification.

Parameter	Value
Resolution:	2560 x 1920 (5MP)
Image sensor:	1/1.8" progressive CMOS
Optics:	Vari-Focal, F1.3-F2.2
Frame rate:	30fps
Field of View (FOV):	45°-84° (horizontal), 34°-62° (vertical)

This network camera generates a video stream in Xvid MPEG-4 video (XVID) encoding. For time synchronization, the current timestamp was additionally superimposed as an image overlay. The IR LEDs for additional illumination in darkness were deactivated in order not to change the visibility of near targets compared to targets further away.

b. Thermal Camera

The thermal camera used has been an Optris PI 640i[3] with specifications listed in Table 2:

Table 2: Thermal camera specification.

Parameter	Value
Resolution:	640 x 480 (VGA).
Detector:	FPA (Bolometer, uncooled, 17µm x 17µm)
Sensitivity:	LWIR, 8-14µm
Focal length:	f=41.5 mm
Frame rate:	32 Hz free run (<=5Hz used in the test)
Field of View (FOV):	15° x 11°

The passive detector converts thermal radiation into image information. If the emissivity is known, a temperature reading for the observed object can be derived from the 16-bit gray values. The self-heating of the camera or detector is corrected by a periodic calibration process. In firefighting, special, robustly designed handheld thermal cameras are used to measure heat generation or to locate people in dark or smoky rooms by their thermal image.

c. Laser Scanner

A RIEGL VZ-400i[4] laser scanner with specifications listed in Table 3 has been used:

Table 3: Laser scanner specification.

Parameter	Value
Standard scan pattern:	„Panorama40“
Field of view (FOV):	100° vertical x 360° horizontal
Standard angular resolution:	0.04° (7 mm point resolution at 10 m distance)
Distance measurements per panorama laser scan:	approx. 22.5 million
3D accuracy of a laser distance measurement:	3 mm @ 50m
Scan time for a "Panorama40" laser scan:	45 seconds, greatly reduced by restricting the FOV

Terrestrial (or static) laser scanning is a three-dimensional measurement technique. The scanner systematically scans its surroundings by deflecting the emitted laser beam with a vertically rotating mirror

[3] optris PI 640i The smallest measuring VGA thermal imager worldwide [26/04/2023]
[4] http://www.riegl.com/nc/products/terrestrial-scanning/produktdetail/product/scanner/48/ [26/04/2023]

and rotating around its azimuth axis, while simultaneously measuring the distance to the object surface and acquiring hundreds of thousands of measurement points per second using the pulse transit time method. Larger areas can be covered by multiple scans from different scan positions. In this work, multiple consecutive laser scans were also acquired from the same position. The field of view and scan resolution were optimized for the measurement task.

The laser source of the RIEGL VZ-400i laser scanner used here emits pulses with a wavelength of 1500nm (infrared) and a pulse length in the order of 1nm. This wavelength is considered "the eye-safe wavelength" because the laser light is almost completely attenuated in water, and thus also in the human eyeball, after only one millimeter of penetration.

d. RADAR sensor

The RADAR sensor (INRAS RadarLog[5]) used in the smoke test is a 77GHz research radar and operates according to the "Frequency Modulated Continous Wave" principle (FMCW) in W-band (4mm wavelength). The RadarLog system is freely configurable within the system limits, and the parameters used in the smoke test are summarized in Table 4. With the chosen configuration, a maximum range resolution (10cm) was aimed for, but this is at the expense of the (unambiguously) measurable range, which is with about 40m significantly below the distance to the last target (therefore only 5 of 10 targets are visible). The data rate for this configuration is about 120MB/s, which is about half of the maximum possible data rate.

Table 4: RADAR sensor configuration.

Parameter	Value	Comment
Bandwidth:	1500 Mhz	Corresponds to a Range Resolution (R_{Res}) of 10cm
Chirp Repetition Interval (CRI):	190µs	Corresponds to a unique velocity range of +/- 5m/s
Samples per chirp:	800	Selected according to R_{max} or R_{Res}
Number of chirps:	512	Corresponds to a resolution of 0.02 m/s
Integration time (TInt):	100ms	Corresponds to a 10Hz range/Doppler measurement
Sampling frequency:	4.44 MHz	Corresponds to a max. distance (R_{max}) of 40m

3. Conducting the smoke tests

On November 15, 2021, two smoke tests were carried out in the "Zentrum am Berg" test tunnel in Erzberg, Austria as part of the ROBO-MOLE research project. The experiments are well documented by videos of the investigated RGB camera and an additional panorama camera positioned in the background.

Due to the sensor technology used, different targets for assessing the visibility were prepared and used in the experiment:

- Ten targets designed for the laser scanner, dimensions 2m x 0.5m, weight about 10kg
- Black & white targets designed for the RGB camera (mounted at two heights)
- Five custom-built thermal targets (black circular targets, electrically heated)

The black & white targets were mounted on the top and bottom of each laser target with adhesive tape (see also Figure 3, right side). The size of the black/white targets was chosen to be 25cm x 25cm to ensure sufficient resolution in the measurement images. The lower area of each target plate was illuminated with battery-powered LED spotlights to provide homogeneous illumination. Every other laser target (Nr. 1, 3, 5, 7, 9) was additionally equipped with a thermal target directly below the upper black/white target. This consists of a matte black aluminum disk (10cm diameter), which can be heated to about 40 °C by means of electrical heating foil and is, thus, clearly visible in the thermal images.

[5] https://inras.at/en/radarlog/ [26/04/2023]

Table 5: Measured distances to laser targets, number of targets per laser target and ambiguity of RADAR measurement.

Target #	Distance	# Black and white targets	# Thermal targets	RADAR R < Rmax
1	15,26m	top, bottom [6]	1	True
2	20,56m	top, bottom	0	True
3	26,20m	top, bottom	1	True
4	31,66m	top, bottom	0	True
5	37,38m	top, bottom	1	True
6	43,19m	top, bottom	0	False
7	49,12m	top, bottom	1	False
8	54,51m	top, bottom	0	False
9	60,24m	top, bottom	1	False
10	65,64m	top, bottom	0	False

The laser targets were positioned approximately 5m apart at a distance of 15-65m from the sensor system in the tunnel (shown as vertical lines in Figure 2). They were arranged in such a way that they could be seen completely by the sensors by using a small lateral offset for each target. At a distance of approx. 5.3m in front of the sensors, the fire cup was located (laterally offset somewhat to the left). On the far right, one can see the people and the sensors. The entire scene was measured directly before the smoke test with the laser scanner with several scan positions. The exact distance of the sensors to the lower black & white targets could, thus, be measured from the laser scan data (see Table 5). The laser targets are also suitable for the RADAR sensor but due to the configuration used, not all of them are within the maximum unambiguously resolvable distance (see last column of table 5).

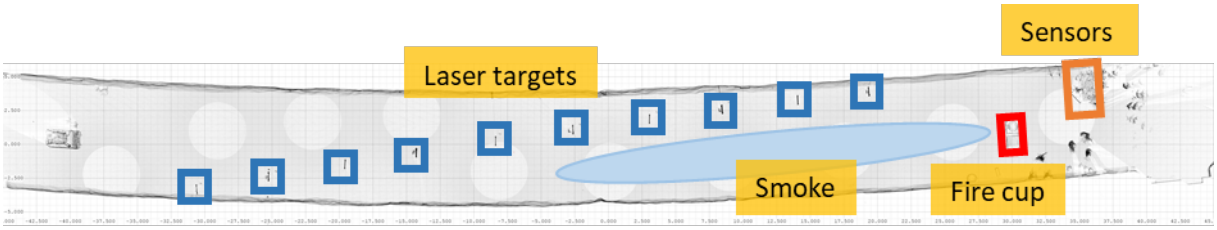

Figure 2: Floor plan of the test setup, point cloud of the composite laser scan (top view).

Figure 3 on the left shows the same scene before the smoke test again as a point cloud from the view of the laser scanner and the adjacent RGB camera (middle). The hot smoke source was a car tire with rim which was burned together with a gasoline/diesel mixture in the burn cup.

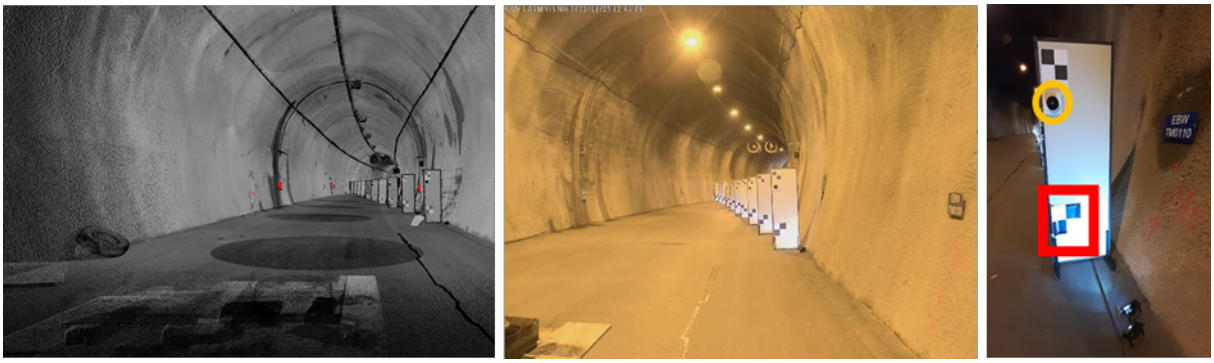

Figure 3: Scene as seen by the sensor system. On the front left the fire cup, on the back right ten laser targets. The detailed view shows the attached black&white targets (red square) and the thermal target (orange circle).

[6] In the evaluation of the RGB camera visibility, only the lower black & white targets have been used.

Figure 4 (left) shows the burn cup during the smoke test and the sensors placed on the right side behind it at a sufficiently large distance. The individual measuring devices are set up as close to each other as possible in order to have the same field of view. For safety reasons, the ventilation was turned on during the smoke test (maximum 2m/s) so that the smoke was diverted away from the sensors in the direction of the laser targes and towards the tunnel portal. Directly next to the measuring equipment was a cross passage to the second tunnel tube, i.e. an escape door for the people present. Protective clothing (helmet, safety vest and safety shoes) was mandatory for all persons.

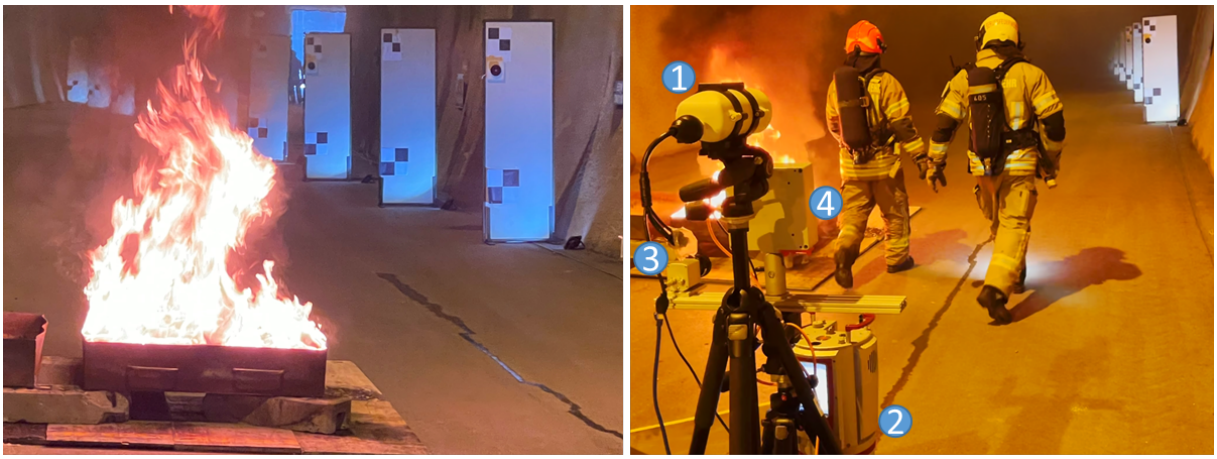

Figure 4: Fire cup and sensor setup: 1-Video camera, 2-Terrestrial laser scanner, 3-Thermal camera, 4-RADAR sensor.

The RGB and thermal video recordings ran continuously during the two tests, and the laser measurements were recorded with an interval of approximately one second. The RADAR measurements had to be limited to short time intervals (samples) due to the amount of data. Since operation (manual start/stop) was not possible in the heavily smoky time sections, these areas are unfortunately not covered by RADAR samples. However, the firefighters wore heavy breathing apparatus and were, therefore, able to move freely in the tunnel at all times during the two tests.

In order to obtain realistic video and meaningful RADAR data (moving objects), they were instructed to move individually or in pairs in the area of the laser targets (also at different speeds, walking or running). However, this unintentionally led to blocking the line of sight to the targets multiple times, which was challenging during the later evaluation of the sensor data.

a. First smoke test

The first hot smoke test took place between about 11:40 and 12:05 in the tunnel "Weströhre Eisenbahntunnel" at ZAB (see Figure 5). At about 11:44:30, a tire was lit in the right-hand of the two fire cups and from about 11:46 to about 11:51, there is a continuous decrease in visibility due to increasing smoke (see also Figure 6), which is of particular interest for sensor comparison. The maximum smoke density is between 11:51 and 11:52, after which the smoke decreases somewhat due to increased ventilation, but the number of visible targets does not begin to increase again until about 11:54, reaching about five targets at 11:55.

Until about 11:58, visibility stagnates or is briefly reduced again and again due to high flames and black smoke passing through. Only then the smoke decreases steadily, so that from about 12:02 all the targets are visible again.

Between approximately 11:48 and 12:01, firefighters (individually or in pairs) repeatedly walked from the position of the sensors back behind the 9th (penultimate) target (marked by dashed red lines in Figure 5). Then, at the end of the experiment, another firefighter walks the course (marked with a solid red line in the diagram). Thus, in addition to the pure visibility measurement, realistic images could be taken with the thermal cameras and, on the other hand, the representation of moving objects (people) in the RADAR measurements could be demonstrated. Unfortunately, the operation of the RADAR sensor was not possible in the phase of maximum smoke, so that no such measurements are available for this period.

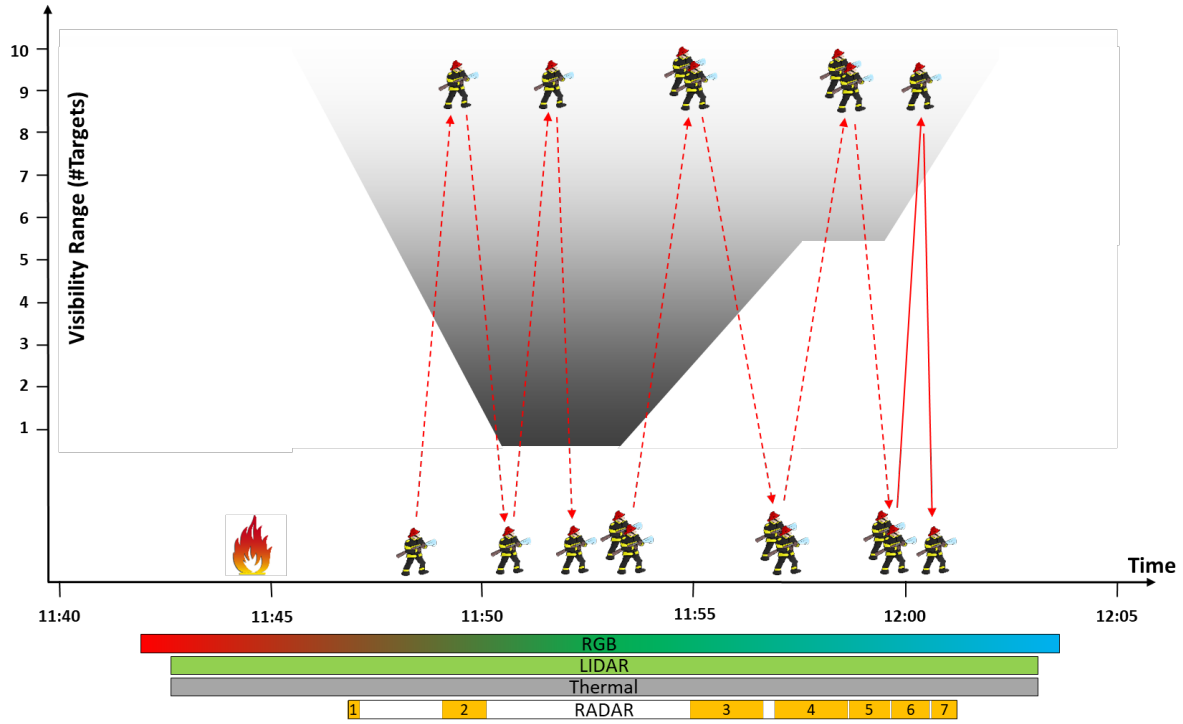

Figure 5: Time graph of the first smoke test including sensor recording intervals. RADAR samples are denoted by numbers.

In Figure 6 below, sample images of the RGB video are shown for a three-minute time interval to provide a first impression of the experiment.

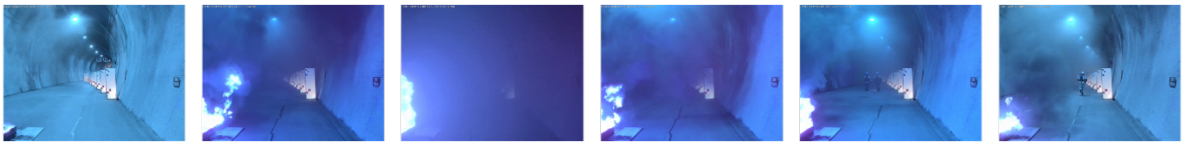

Figure 6: Recordings of the RGB camera at the times 11:45 to 12:00 at 3min intervals from left to right (first smoke test).

b. Second smoke test

The second hot smoke test took place between 12:49 and 13:05 (see figure 7 below). As in the first test, a tire was lit in a gasoline/diesel mixture (this time, however, in the left of the two fire cups, i.e., about 1m away from the direct line of sight between the sensors and the laser targets). Compared to the first smoke test, the smoke increased much faster from about 12:53:45 and reached a maximum just less than a minute later (about 12:54:30 to 12:55:35). The intensity, though, turned out to be somewhat lower than in the first test, and the first laser target always remained visible.

From about 12:55:35 the smoke is blown out and visibility slowly improves to about four targets, but then stagnates due to the high flames and the fire continues to smoke heavily. From about 12:56:30 the visibility deteriorates again, for a short time only the first target is visible (about 12:57). At about 12:58 the fire cup is cooled with some water on the side. Afterwards, visibility improves, but remains limited to about three targets until about 13:00 (strongly fluctuating depending on the smoke passing through), after which one more target becomes visible.

Only after about 13:01 the visibility improves sustainably, at about 13:02:30 all of the targets are visible. At about 13:03, the fire is finally extinguished with water, which produces a lot of water vapor and temporarily reduces visibility to only about four targets. From approx. 13:04:30, all the targets are visible again, and from approximately 13:05, the entire tunnel in the area of the targets is smoke-free again.

Also during the second smoke test, firefighters moved in the area of the laser targets (from approx. 12:51:45 until 13:02), they are recorded in RADAR samples #8 - #12.

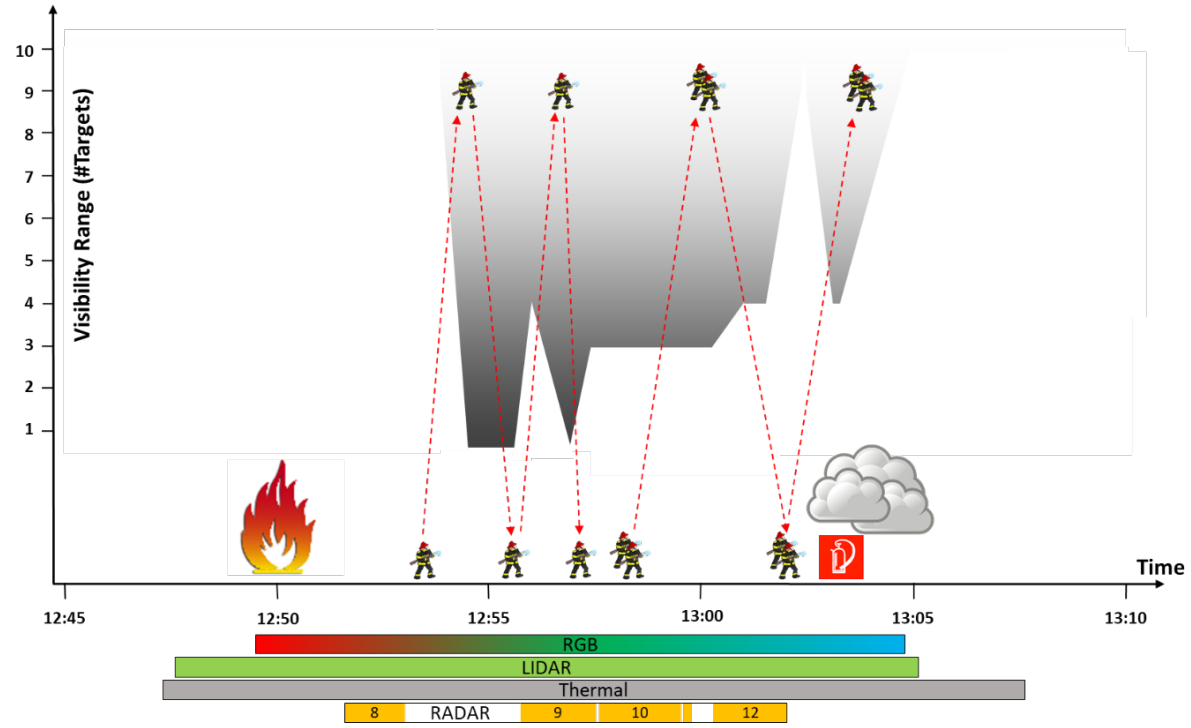

Figure 7: Time graph of the second smoke test including sensor recording intervals. RADAR samples are denoted by numbers.

As for the first hot smoke test, the recordings of the RGB cameras can be examined to get an impression of the smoke intensity and distribution at any time during the experiment. Figure 8 shows sample images from the video at a three-minute time interval. Figure 9 shows a laser scan performed during the test.

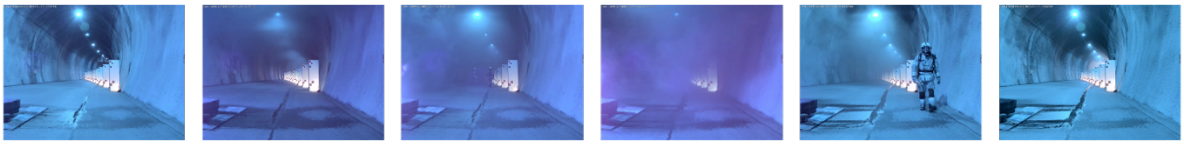

Figure 8: Recordings of the RGB camera at the times 12:50 to 12:05 at 3min intervals from left to right (second smoke test).

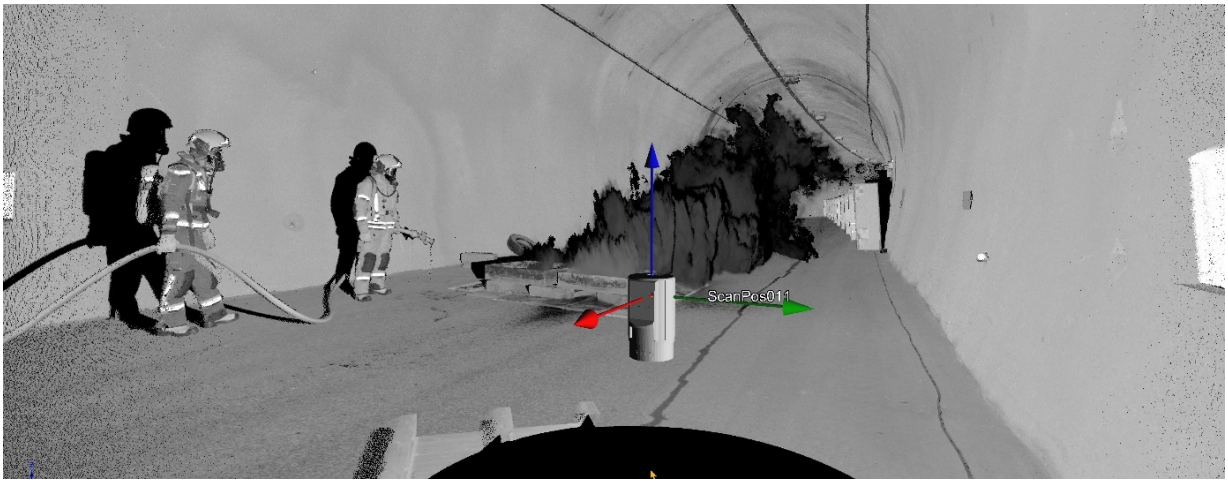

Figure 9: High resolution laser scan perfomed during the test, the hot smoke is clearly visible as part of the 3D point cloud.

4. Evaluation

To compare the visibility of each sensor, the number of visible targets was determined. While the RMS contrast was used for the RGB and thermal cameras to determine the visibility, the evaluation of the laser scans was based on a projection of the 3D point data onto the ground plane and subsequent image analysis. In the following, the preparation of the data and the methods for visability determination are described in more detail.

a. Overview over data sets recorded

The following table gives an overview of the sensor data (RGB and thermal image data or scan data) recorded continuously during the smoke tests. The times given are not (yet) synchronized with each other, this step is described in more detail below.

Table 6: Start and end times of the continuously recorded sensor data.

Sensor	Start	End	Smoke test
RGB	11:41:20	12:02:50	#1
LiDAR	11:33:17 (not synchronized)	12:03:08 (not synchronized)	#1
Thermal	11:42:08 (not synchronized)	12:02:36 (not synchronized)	#1
RGB	12:49:30	13:04:49	#2
LiDAR	12:47:21 (not synchronized)	13:07:41 (not synchronized)	#2
Thermal	12:47:41 (not synchronized)	13:05:06 (not synchronized)	#2

While the RGB image data was recorded at a fixed frame rate of 30Hz, the frame rate of the 16bit thermal images was variable and dropped (unintentionally) from about 5Hz initially to below 2Hz due to performance reasons during recording. The data from the RGB camera are available as RGB video data stream. The videos are recorded with a resolution of 2560x1920 pixels with MPEG-4 Visual (XviD) encoding and 11.6Mb/s.

With the laser scanner, scans were taken periodically. The angular range was limited to those directions where the laser targets were located, see configuration parameters listed below.

Table 7: LiDAR configuration.

Parameter	Value
Number of measurements/scan:	Approx. 700,000 (2512 vertical x 276 horizontal)
Scanned angular range:	vertical +60° / -40° horizontal 11°
Angular resolution:	0,04° (7mm@10m)
Scan time:	Approx. 1 second
Scan mode:	sequence (clockwise, counterclockwise, alternating)
Number of scans:	Smoke test 1: 1078, smoke test 2: 735

For the first smoke test, 1078 individual scans were taken every second in the manner described, and 735 for the second. Each scan is time-stamped (date / time). Figure 10 shows a single scan from the scanner's point of view (2D View), from a freely selectable perspective view (left figures) and in the orthogonal view from above (right figure). In the latter, the laser targets and a firefighter on the far left appear in white, and the point cloud without a ceiling is shown in red.

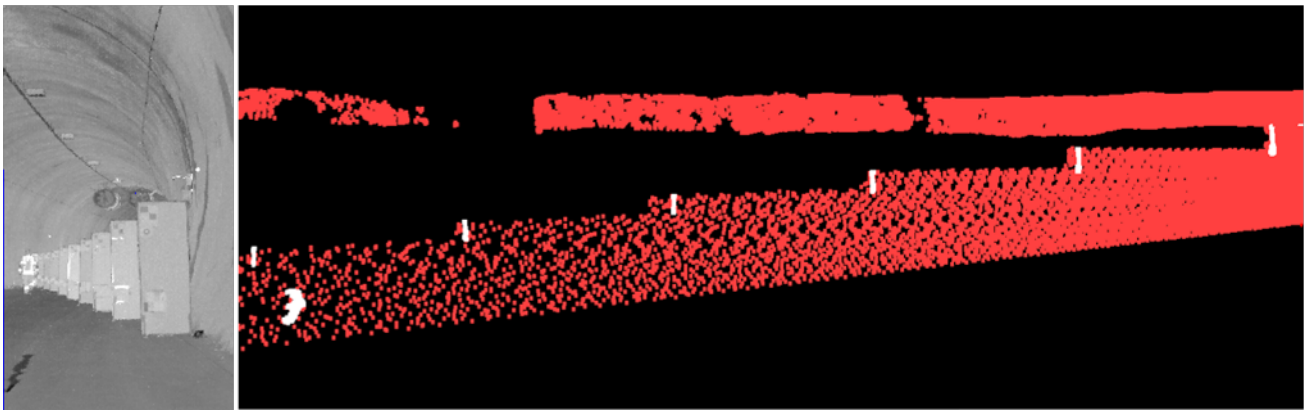

Figure 10: Single scan, approx. one second scan time, 0.04° angular resolution (left side), orthogonal top view (right side).

Unlike the other sensors, only short RADAR samples were recorded due to the large amount of data, the following Tables 8 and 9 provide an overview of the raw data recorded during the two smoke tests:

Table 8: Overview of RADAR samples during the first smoke test.

#	Start	End	Data Set (raw data)	Volume
1	11:46:19	11:46:43	tunnel_20211115114619.h5	2.6 GB
2	11:48:44	11:49:45	tunnel_20211115114844.h5	7.1 GB
3	11:54:21	11:56:04	tunnel_20211115115421.h5	12.1 GB
4	11:56:22	11:57:58	tunnel_20211115115622.h5	11.3 GB
5	11:58:05	11:59:04	tunnel_20211115115805.h5	6.9 GB
6	11:59:10	11:59:54	tunnel_20211115115910.h5	5.1 GB
7	12:00:00	12:00:39	tunnel_20211115120000.h5	4.3 GB

Table 9: Overview of RADAR samples during the second smoke test.

#	Start	End	Data Set (raw data)	Volume
8	12:51:42	12:53:00	tunnel_20211115125142.h5	9.2 GB
9	12:55:46	12:57:30	tunnel_20211115125546.h5	12.3 GB
10	12:57:37	12:59:24	tunnel_20211115125737.h5	12.6 GB
11	12:59:32	12:59:47	tunnel_20211115125932.h5	1.4 GB
12	13:00:23	13:02:05	tunnel_20211115130023.h5	12.1 GB

b. Data preparation

For processing, one RGB frame per second is extracted from each video and saved as an image file. The exact time of individual frames in the video is determined via the time overlay using OCR.

In another preprocessing step, the 16bit images of the thermal camera were converted to 8bit images using a fixed conversion (gray values between 1114 and 1311 were mapped to the values [0,255] representing a temperature range of 11.4 to 13.1°C). For simple visual analysis, despite the mentioned non-constant frame rate, video files with a fictitious frame rate of 5 Hz were calculated from the 8bit thermal images. For this reason, the thermal videos cannot be directly synchronized with the RGB videos. However, individual thermal images can be precisely assigned in terms of time due to the time stamp they contain.

In order to be able to evaluate the individual laser scans automatically with regard to visibility, two-dimensional orthogonal views were generated from the individual scans. Points of the invariant part of the point cloud (tunnel wall) were colored red, and points of the current detail scan (including the laser targets) were colored white, as shown in the following illustration (Figure 11). The floor and ceiling of the tunnel were masked out for the 2D representation, and the laser target themselves were captured in their entirety (full height). In the lower right corner of the resulting images in JPG format, the date and time of capture were superimposed.

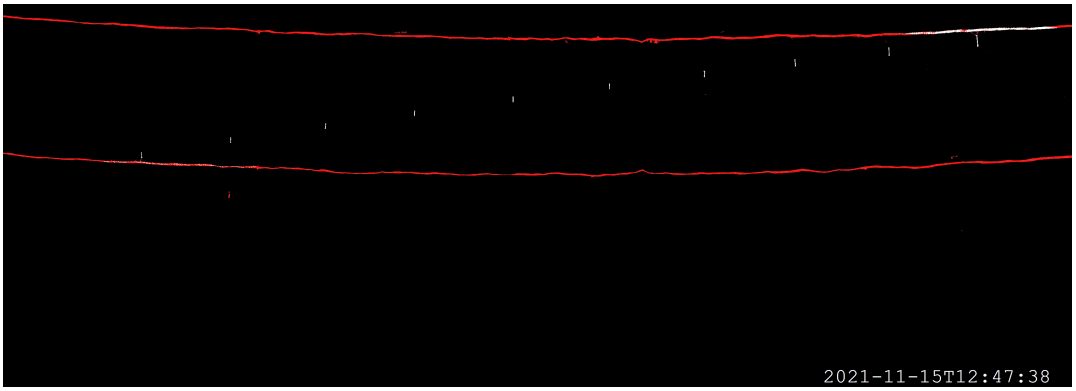

Figure 11: Individual scan (white) and common point cloud of the tunnel (red), orthogonal view from above.

Due to technical problems, the synchronization of the sensors did not take place exactly as planned via a common time server and, therefore, had to be estimated afterwards with respect to the reference time (time stamp in the RGB video) on the basis of identical contents to an accuracy of +/- 0.5s.

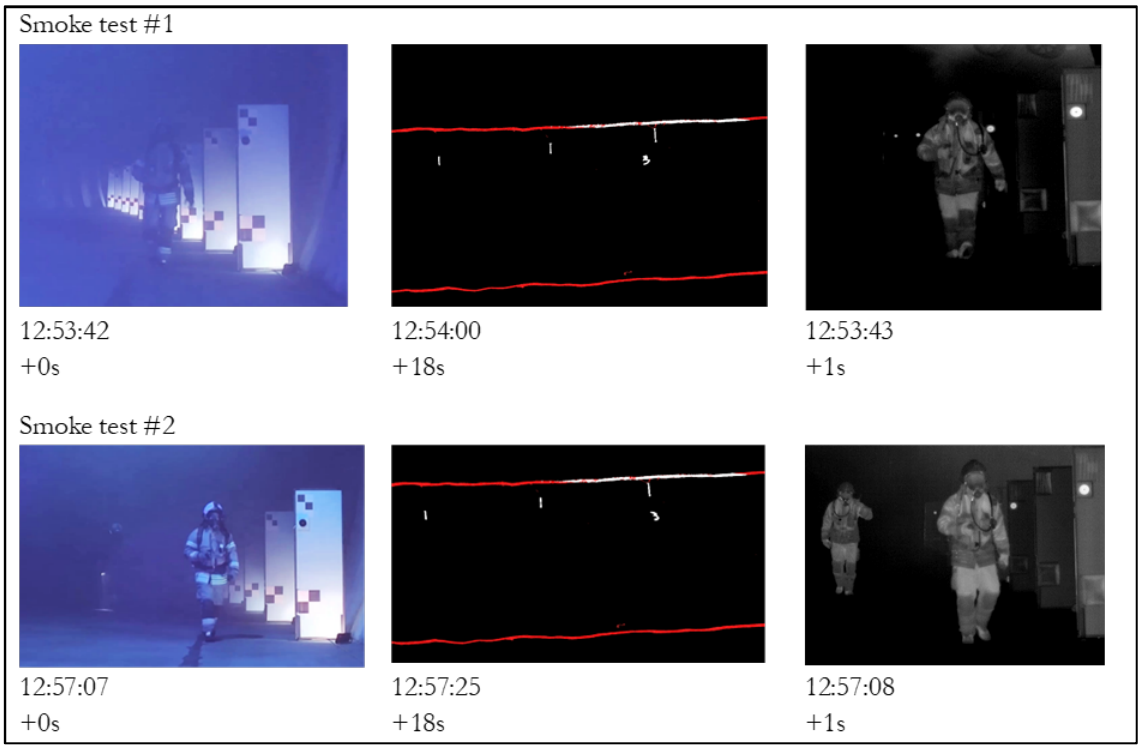

Figure 12: Estimation of the temporal offsets of the sensors with respect to the RGB video.

For each smoke test, several scenes were selected that show unique situations and were equally captured by each sensor. One such situation is shown for each smoke experiment in Figure 12 above. The position of the firefighter directly next to the first laser target can be seen in each sensor image. For both smoke tests, identical offsets have been determined (positive values denote a leading time). The thermal camera and the RADAR sensor ran on the same laptop and therefore have the same time offset (+1s) but the LiDAR has a relatively large offset of +18s. The time difference between each sensor was taken into account in the joint analysis.

c. Determination of visual range in the RGB images

The determination of the line-of-sight range at a certain point in time is based on the visibility of the individual targets. This in turn is determined based on the measured contrast of the respective black and white target. First, areas of each black&white target (checkerboard pattern, bottom target) were extracted from the RGB image. The size of the checkerboard pattern was chosen so that the most distant target was

still imaged at a sufficiently high resolution of 16x16 pixels to allow the contrast to be determined. Figure 13 shows the cropped targets.

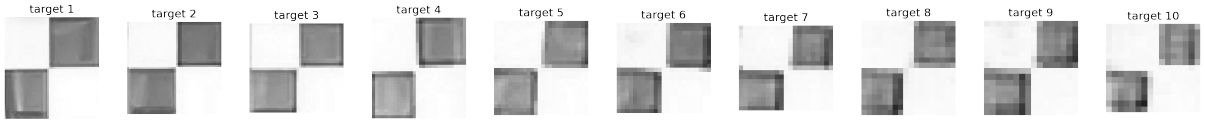

Figure 13: Extracted black & white targets of the laser targets 1-10 (not affected by smoke).

As a measure for the contrast of a target we used an RMS value calculated using the standard deviation of the pixel intensities:

$$c_k = \sqrt{\frac{1}{M * N} * \sum_{i=1}^{M} \sum_{j=1}^{N} (I_{ij} - \bar{I})^2}$$

where c_k is the contrast of the k[th] target, M, N denotes the image size, I_{ij} the intensity of the pixel (i, j), and $\bar{I}$ the mean intensity of the target.

Visibility of a target is determined by using thresholds for the measured contrast. When the contrast is high, a target is declared visible, and when the contrast is very low, it is declared invisible. The threshold below which a target is no longer visible was determined empirically and set as the RMS contrast $c_{th} = \frac{5}{255} = 0.0196$. At this contrast, the pattern is just visible to the human eye. Thus, the maximum contrast that can be achieved is 0.5. Visible targets are therefore those for which $c \geq c_{th}$ holds. Figure 14 shows as an example the black & white targets (tunnel was filled with smoke) where the first three targets have sufficient contrast (target 1-3) and the others having too low contrast (target 4-10) to recognize the black and white pattern any more.

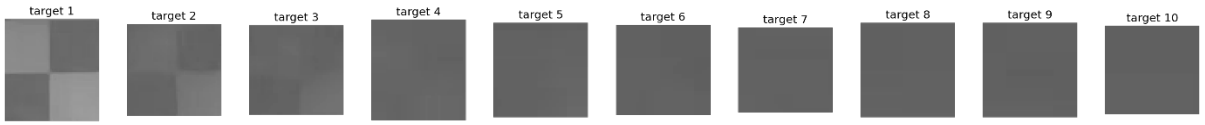

Figure 14: Black & white targets at the time 12:55:11 (heavy smoke) with contrast values (multiplied by 255): 19.32, 8.11, 4.82, 1.67, 1.94, 1.49, 0.70, 0.95, 0.97, 1.05

The visibility range at a given time is given as the number of targets visible:

$$v = \sum_{z=0}^{Z} \begin{matrix} 1 & if\ c_z \geq c_{th} \\ 0 & else \end{matrix}$$

Where v is visibility range, Z is number of targets, and c_z is contrast.

d. Determination of the visual range of the thermal targets

Since RGB camera and thermal camera both provide image-based data, the same method for contrast measurement was applied for the thermal targets. Figure 15 shows the extracted thermal targets when no smoke was present and Figure 16 when visibility in the visual spectrum was greatly degraded by smoke (compare also with Figure 18). One can see that the contrast is not too much affected by smoke in this part of the spectrum (LWIR).

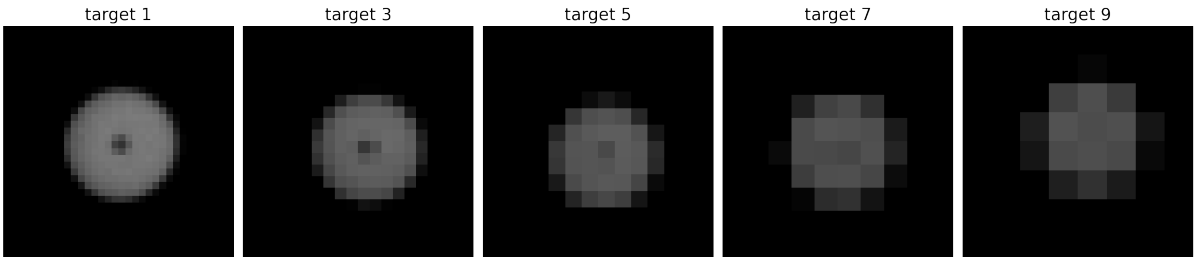

Figure 15: Extracted thermal targets of the laser targets 1, 3, 5, 7, 9 (no smoke present).

The contrast is determined by an RMS contrast value same as for the RGB images. The threshold for visibility was empirically determined as $c_{th} = \frac{5}{255} = 0.0196$ (same as for RGB images as again the contrast should be recognizable by human eye).

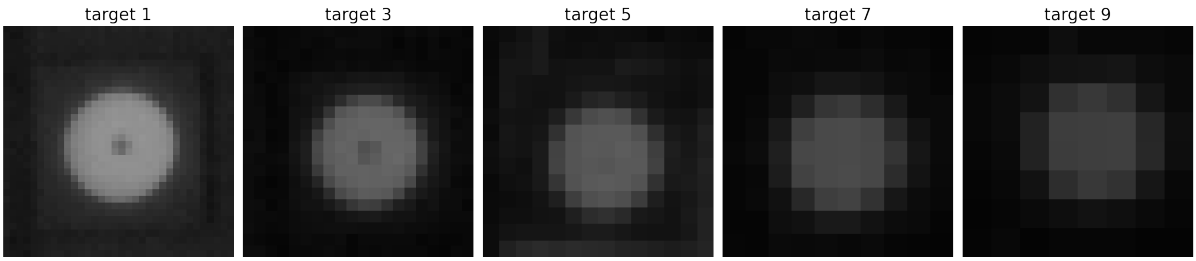

Figure 16: Contrast for thermal targets 1-9 at time 12:55:11 (heavy smoke) with contrast values (multiplied by 255): 39.6, 30.2, 23.7, 22.4, 19.0

e. Determination of the visual range in the laser scans

In contrast to the evaluations of the image-based sensors, visibility was calculated based on two-dimensional orthogonal views (floor plans) from the detail scans, which have been prepared as described before for each scan. To determine the visibility of the laser targets from those 2D views, the "pixel activity" in the corresponding area was assessed. A specific pixel in the 2D view is considered „active“ if at least one 3D point was projected onto that pixel. Subsequently, a target was defined as visible if the number of activated pixels reached at least 50% of the median value for the corresponding target area. In the example below, all ten laser targets are visible at time t=12:47:38.

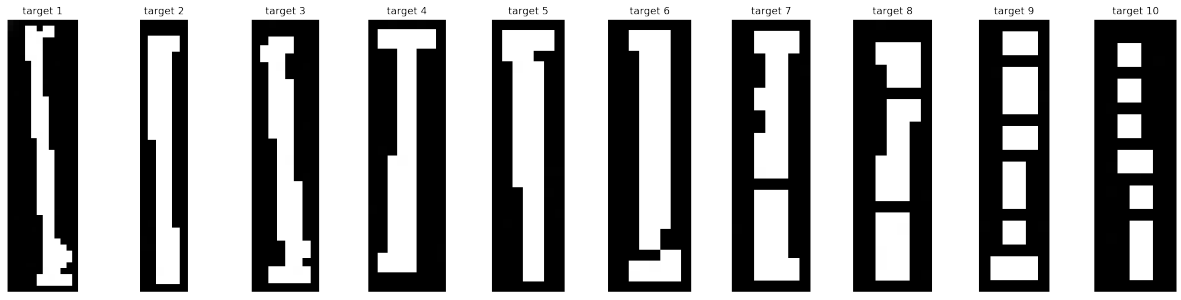

Figure 17: LiDAR targets 1-10 in orthogonal projection from above (top view).

f. Evaluation of the RADAR data

For the recorded raw RADAR data, so-called Range/Doppler (R/D) maps were calculated in post-processing with a frame rate of 10Hz. The R/D maps cover the range up to 40m and the velocity range of +/-5m/s within a FOV of about 100° in front of the sensor. Larger distances (up to about 150m) could be achieved at the expense of spatial resolution if configured appropriately. However, an evaluation of the RADAR visibility as performed for the other sensors does not seem to make sense since the first five laser targets are continuously visible as static targets. A further analysis of the extent to which the intensity values in the R/D maps are influenced by smoke has not been carried out.

5. Results

The central part of this work is the direct comparison of the "visibility range" or "target visibility" of the individual sensors. The visibility of a target is defined as follows:

Table 10: Definition of visibility or line-of-sight range of the sensors used in the described experimental setup.

Sensor	Definition of Visibility / Visibility Range
RBG or thermal camera	The target is still visually visible in the image if the contrast exceeds a defined threshold.
LiDAR	The corresponding target is still visible in the point cloud displayed and measured orthogonally from above, if the number of active pixels (at least one 3D point was projected onto this pixel) exceeds a threshold value.
RADAR	The target stands out significantly in the range-Doppler diagram as an object at the appropriate distance and with v=0 (static object) above the signal noise. The unambiguous distance range is limited to about 40m, targets at greater distance are displayed incorrectly (mirrored with respect to R_{max})!

Since both smoke experiments are highly dynamic processes, time synchronization is particularly important for direct comparison. The common start times for the evaluation of all sensor data are:

- Smoke test #1: t=0: 2021-11-15 11:33:00.
- Smoke test #2: t=0: 2021-11-15 12:47:00

a. Direct comparison of the sensors

According to the above definition, the visibility ranges for all sensors were determined. Figure 18 shows the result of the visibility range determination for RGB camera, LiDAR scanner and thermal camera over time (RGB camera: blue, thermal camera: red, LiDAR: green) in the first smoke experiment. The visibility range indicates how many targets are visible at each point in time. A value of 0 means that no target was visible at that time. The last thermal target is located on laser target number 9 (so the value 10 cannot be reached by the thermal camera).

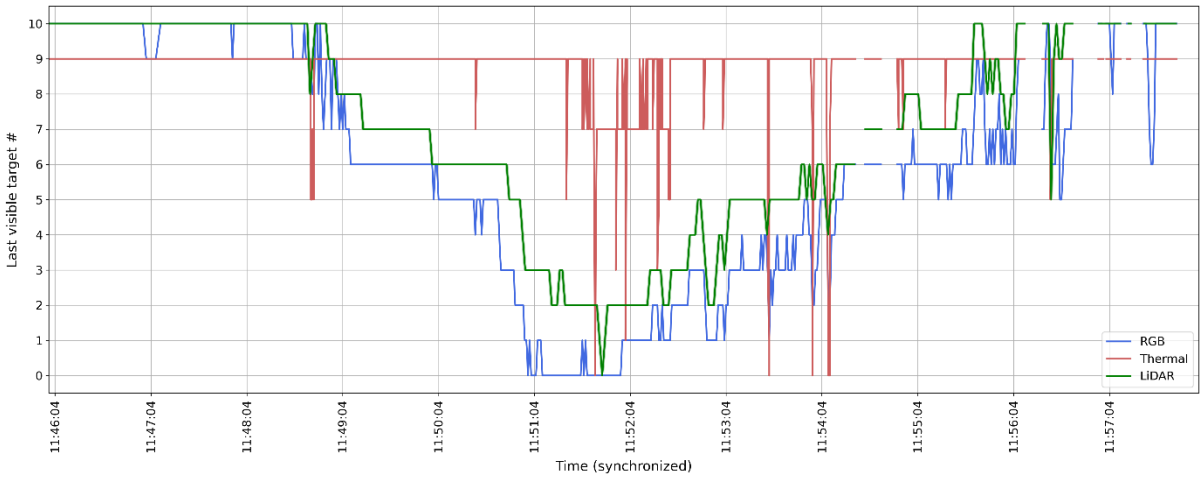

Figure 18: Visibility of all three sensors in the first smoke test with number of the most distant visible target.

It can be seen that the laser scanner was able to penetrate the smoke about one target (i.e. about 5 meters) further than the RGB camera. The rapidly increasing smoke dramatically reduces the visual range of both sensors within minutes or even seconds. The thermal camera was almost always able to detect all thermal targets regardless of smoke development but severe drops in visibility can be seen at some times. This may be caused by people (firefighters) passing through, or, starting at 11:51:00, by isolated flames or hot plumes of smoke appearing in front of the thermal target (see also Figure 23). Since the black & white targets were located at a lower position on the target panel, they were generally less obscured by the smoke plumes.

In comparison, Figure 19 shows the course of visibility in the second smoke test. Here, the visibility of the LiDAR breaks down a little earlier than that of the RGB camera, which may be due to a different smoke distribution or to the significantly higher dynamics (smoke increase within a few seconds).

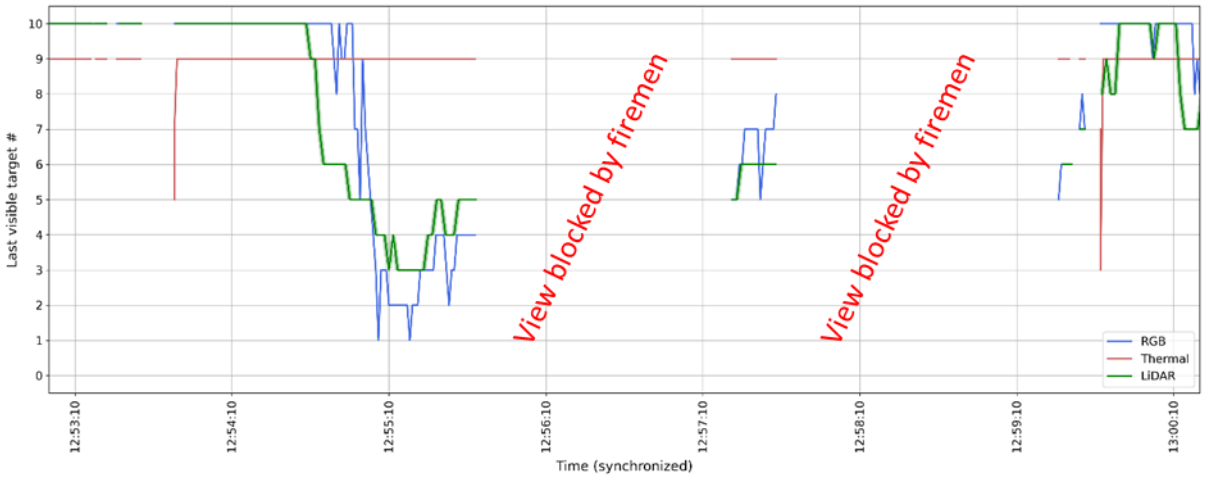

Figure 19: Visibility of all (three) sensors in the second smoke test with number of the most distant visible target.

Unfortunately, due to the large number of persons, there were significantly more false measurements in the second test, which had to be masked out in the evaluation. In the following, the individual sensors and their special features will be discussed in detail.

b. Laser scanner

To describe the rapidly reduced measurement range, the following table shows the result of the automated visibility analysis of the laser targets for the first smoke test. One can see the highly dynamic behavior: Three minutes after the first laser target is no longer measurable for the laser scanner, no target can be seen any more. The visibility is thus reduced by 50 meters in three minutes and at the end, the visibility for the human eye is less than 15 meters.

Please note that the fire source itself is about 5.3 meters away from the laser scanner and that this space has not always been completely filled by smoke (e.g. in the second test, when a stronger ventilation was used). That means that visibility of a certain target does not always mean exactly the same distance affected by smoke (absolute visibility range). On the other hand, due to the position of all sensors at the same location they can always be compared relatively to each other.

Table 11: Result of the visibility analysis for the laser scanner for smoke test 1.

TLS Time	RGB Time	Target disappears	equals distance [m]
11:49:07	11:48:49	10	65,637
11:49:17	11:48:59	9	60,237
11:49:34	11:48:16	8	54,507
11:50:12	11:49:54	7	49,121
11:51:05	11:50:47	6	43,185
11:51:14	11:50:56	5	37,377
11:51:15	11:50:57	4	31,658
11:51:24	11:51:06	3	26,200
11:51:44	11:51:26	2	20,559
11:52:02	11:51:44	1	15,260

The following figure shows one individual scan (viewed from the side) in which the laser scanner can detect only six laser targets. All the others are already covered by smoke and can therefore no longer be detected. However, since the laser scanner is multi-target capable, multiple echoes can be received per transmitted laser pulse. The point cloud was colored here according to the echo class:

- green dots: Echoes from "single targets" (i.e., only one echo per transmitted laser pulse).
- yellow dots: echoes of "first targets" (since obviously more were detected)
- blue dots: Echoes of the "last targets“

In this example one can see that the hot smoke cloud (yellow part) can be identified (and thus, eliminated) well in the laser scan. In addition, at the sixth laser target (far left), one can see that the lower part of the (2m high) laser target is still well measurable for the laser scanner, while the upper part slowly "disappears" in the smoke. This can be explained by the fact that hot smoke rises. A laser scanner should therefore be positioned as far down as possible in a smoke-filled tunnel.

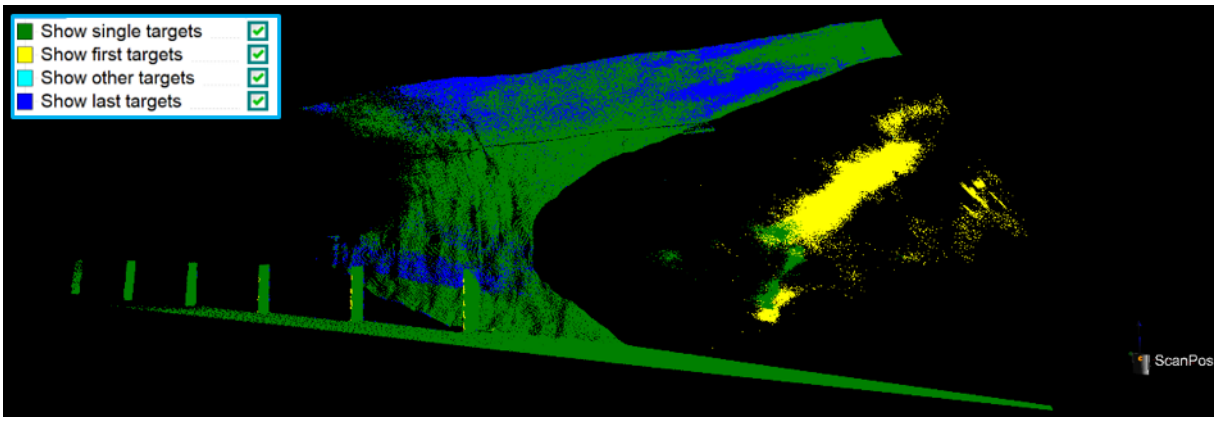

Figure 20: Point cloud of a detail scan, colored according to the class of the laser scanner's multi-target capability. Laser scanner on the right. Laser target on the far left to center.

As the smoke increases, the scatter of the range measurement also increases, the laser targes become "brighter" in the orthogonal top view. In the case of very dense smoke (e.g. caused by short fire bursts), multiple echoes are returned, but due to the scanner's multi-target capability, the laser targets behind are often still visible (see Figure 21).

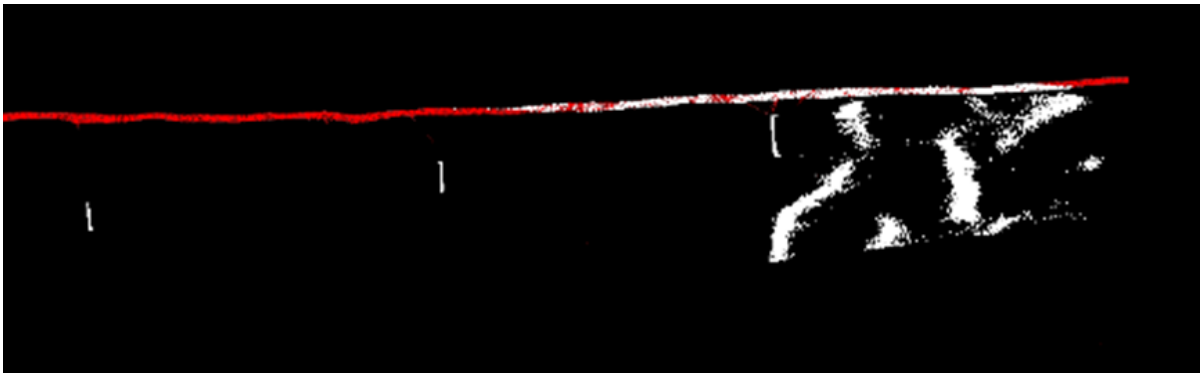

Figure 21: Laser scanner sees multiple echoes (dense smoke and laser targets behind, t= 13:03:57).

c. Thermal camera

In the images of the thermal camera, thermal targets applied to every other laser target are visible most of the time (even at times with maximum smoke). Individuals are also clearly visible and can be tracked over the full distance observed (70m).

Figure 22 shows the same point in time in the RGB and thermal images respectively. One has to consider that the field of view of the thermal camera (marked by a red rectangle) is much smaller than of the RGB camera. That means that hot smoke from the fire on the left is cooling down significantly before entering the field of view of the thermal camera somewhere in front of the first laser target. Consequently, the firefighter walking at the level of the 5th laser target is well visible in the thermal image, but not visible in the RGB image.

Figure 22: Comparison of a scene in the RGB and thermal image (t=11:49:03).

On the other hand, there are also brief glares of the thermal camera when very hot smoke passes directly in front of the camera (see Figure 23). These interruptions in visibility are also visible in the contrast measurements as short-term disturbances.

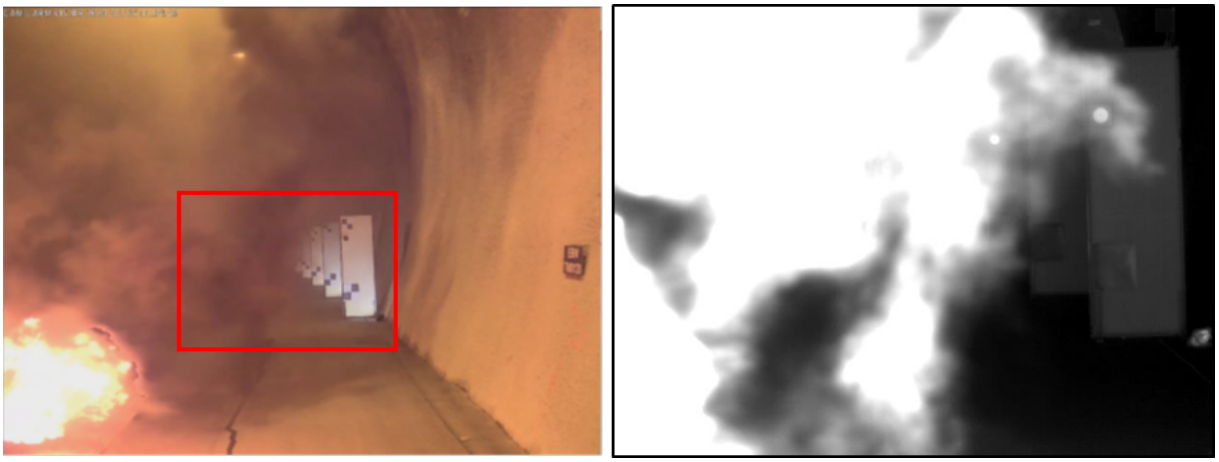

Figure 23: Glare of the thermal camera due to stinging flames or hot smoke in the foreground (t=11:54:43).

On the 5th laser target, a part of the metal frame was exposed, which led to a strong reflection (see Figure 24). Since this strong reflection was very disturbing, especially for the contrast measurement of the thermal target directly next to it, the metal frame was taped off before the second smoke test.

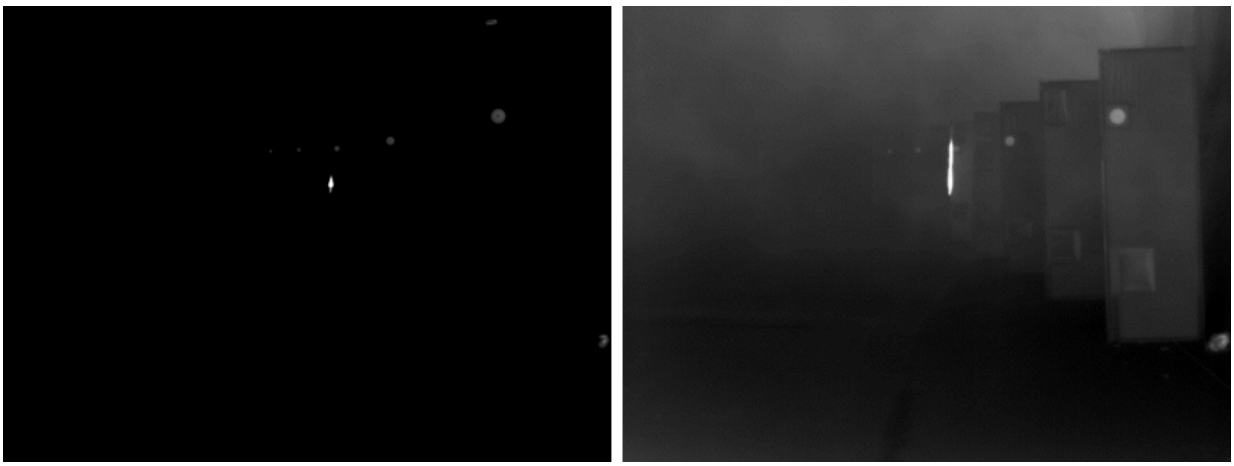

Figure 24: Comparison of the thermal images shortly after ignition (11:45) and at maximum smoke (approx. 11:52)

However, with the applied constant conversion of the 16 bit images to 8 bit, images at very different times can also be compared (see again Figure 24). Here, on the one hand, it can be seen that the round thermal targets (on laser target 1,3,5,7,9) are always visible, but the contrast is somewhat reduced due to the smoke (more detailed analysis below). In addition, there is an interesting effect that the laser targets itself are (almost) invisible at first because they have the same temperature as the environment. Later, due to the heating by the warm air and the reflection of the thermal radiation the laser targets are well recognizable.

The following figures show in detail the course of the contrast and brightness of the five thermal targets in the first smoke test.

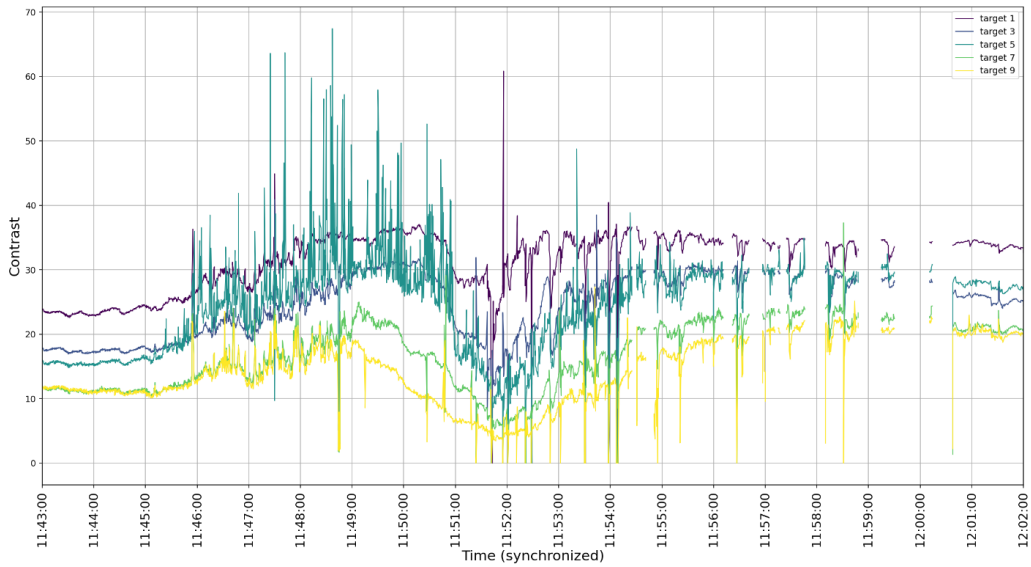

Figure 25: Contrast measurement of the thermal targets in the first smoke test.

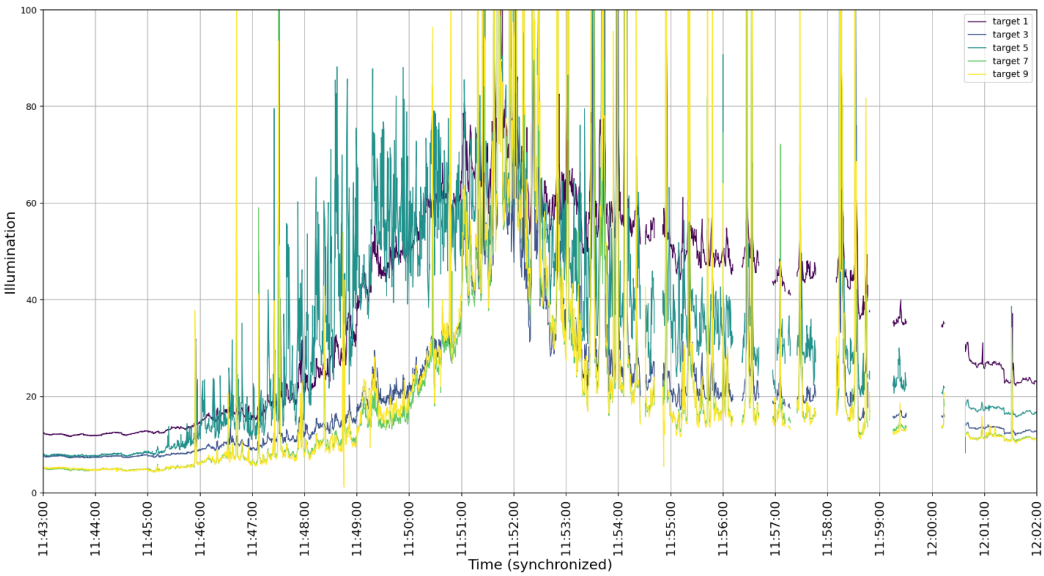

Figure 26: Average brightness of the thermal targets in the first smoke test.

It can be seen in Figures 25 and 26 that the contrast decreases slightly due to the hot smoke at the peak of the experiment between 11:51 and 11:52, but the brightness increases. This can be explained by the increasing heat from the fire reflected by the targets as thermal radiation. At target #1 (at the distance from the fire of about 10m) the increase is particularly strong, at the more distant targets #3, 7 and 9 it is almost identical. Target #5 is very noisy in the measurement due to the problem described above with the neighboring highly reflective metal surface.

e. RADAR

As a result of processing the raw RADAR data, Range/Doppler maps with a frame rate of 10Hz were obtained. These are retrievable as videos and can be displayed e.g. synchronized with the RGB video to facilitate interpretation. Static targets (tunnel wall, laser targets) map themselves on the vertical v=0 line. The first five laser targets are easily recognizable at the expected distances, the remaining targets are outside the unambiguous range (40m). No noticeable degradation due to smoke can be visually detected for the first five targets, but a more detailed analysis of the intensity values has not been performed.

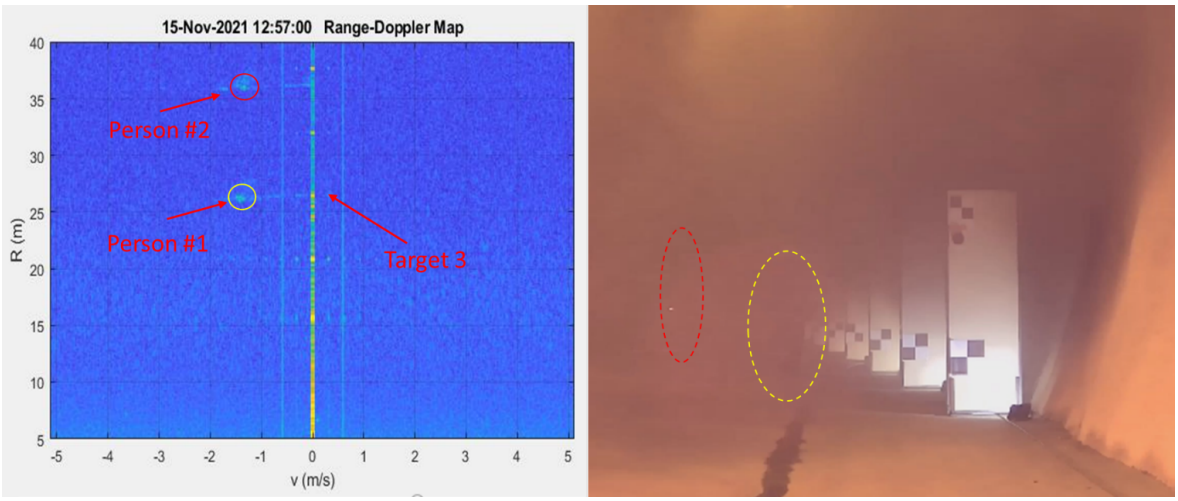

Figure 27: Range/Doppler map and corresponding RGB image of a scene in the second smoke test (t=12:57:00).

Moving objects (people) are clearly visible in the Range/Doppler Map, objects with negative relative velocity are shown to the left of the vertical v=0 line (approaching objects), objects moving away from the sensor are shown to the right. In Figure 27, two approaching objects (firefighters) with approximately the same walking speed can be seen at about 26m at the level of the 3rd laser target and about 36m (in front of the 5th laser target). In the RGB image taken at the same time, the firefighters are practically not visible (dashed red/yellow markings).

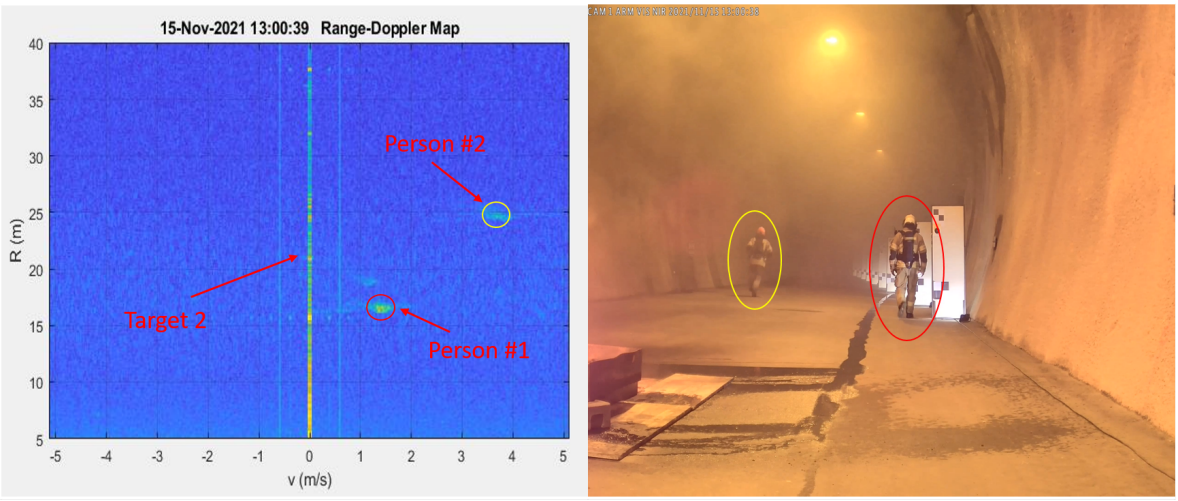

Figure 28: Range/Doppler map and corresponding RGB image of a scene in the second smoke test (t=13:00:39).

In Figure 28, one can see an object (a walking person) moving away at the level of the 1st laser target, a second person is running away from the sensor at about 4m/s at the level of the 3rd laser target. By analysis of the "Micro-Doppler signature" (not done here) it's also possible to distinguish between persons walking or running and other objects with similar RADAR cross section and speed (slowly moving vehicles).

6. Conclusions

The following interpretation of the results is carried out in two parts: at the beginning each sensor is evaluated separately and then a comparison of the different sensors is done. In general, it can be concluded that hot smoke has a significant influence on the measurement range in some cases.

- RGB cameras provide immediately understandable information in good visibility, but no direct distance or speed measurement. Visibility is greatly reduced by smoke, depending on its density. Since this is a passive measurement method, active illumination of the scene is necessary even in a smoke-free tunnel.

- A laser scanner (LiDAR) is an active sensor because it emits laser pulses that can be used to directly measure distances to the tunnel wall and other objects. It therefore works in principle even in an unlit tunnel. The wavelength of the laser pulses is in the infrared, i.e. invisible, range for various reasons. On the one hand, this means that the human eye is not dazzled, and on the other hand, the laser class 1 (eye-safe) can be maintained at the eye-safe wavelength of 1550 nm. Increasing the laser power is not helpful, as it jeopardizes laser safety and does not significantly increase the measurement range due to hot smoke. With the multi-target capability and the detailed analysis of the received laser pulses, the range can be (slightly) increased in hot smoke but erroneous measurements are to be expected with reflections in the smoke-filled air. These can be largely eliminated automatically up to an acceptable smoke density by suitable filtering (e.g. the "last target" in multi-target detection, or filtering according to the shape of the backscattered laser pulses).

- A thermal camera measures heat radiation passively, i.e. it does not need any illumination, thus e.g. persons in dark/cold tunnels are easily visible. Metal objects reflect thermal radiation very well or stand out well from the background (tunnel wall) due to their individual emission coefficient. Visibility generally was not too much affected by hot smoke unless the line of sight is directly blocked by very hot smoke (next to a fire).

- RADAR sensors actively measure velocities and distances with high accuracy, these measurements can be visualized as so-called Range/Doppler maps. However, only one directional component (generally the horizontal angle) can be measured, and the accuracy is rather low (a few degrees). However, there is a very high potential for detecting moving objects (people, vehicles) in poor visibility.

The differences between the individual sensors are sometimes considerable. They are summarized in the following table:

Table 12: Comparison of the tested sensors.

	RGB camera	Laser scanner	Thermal camera	RADAR
Influence of hot smoke on range:	strong	strong	low/sporadic	very low
Distance measurement:	no	yes	no	yes
Speed measurement:	no	indirect	no	yes
Active illumination necessary:	yes	no	no	no
Angular resolution / single measurement:	0,018°	0,04°	0,023°	~3°
Result:	2D	2D / 3D	2D	2D (R/v)
Price:	low	high	low	medium

As can be seen in Figure 18 and 19, the reduction in visibility at different smoke densities is greatest for the RGB camera. The laser scanner can measure a little further, but only a few meters. As a rule of thumb, one can say that a laser scanner can measure just a little further than the human eye through smoke. The greater advantage, however, is that no external lighting is required. The thermal camera is only significantly disturbed or blinded in direct vision by very hot smoke or stinging flames, and the RADAR sensor seems to be the least affected one (although here only a purely qualitative investigation was carried out and only half the distance (40m) was considered). The authors are aware that the conclusions above are based on just one specific RGB- and thermal camera model, LiDAR and RADAR system. Using e.g. different wavelengths or measurement principles might give different results.

For practical use, the combination of all tested sensors seems to make sense in order to be able to use the individual strengths. Possible applications are:

- Navigation of a robot in a tunnel filled with smoke or
- three-dimensional survey of a tunnel after an accident.

For both cases, it is advisable to mount the sensors low on a mobile platform, since hot smoke is known to rise and visibility conditions are best just above the road surface. However, in order for such sensors to actually be used in practice, they must be designed to be "smoke-proof." This ranges from protective housings against smoke and heat to cleaning the aperture of the measuring devices.

7. Acknowledgements

This research has been funded by the Austrian security research program KIRAS of the Federal Ministry of Finance (BMF). Project number: 879693 (ROBO-MOLE).

The corresponding author wants to thank his co-authors for the exellent cooperation within the research project, their valuable contributions and patience to get the paper finalized.

Publication bibliography

Fritsche Paul; Kueppers Simon; Briese Gunnar; Wagner Bernado (2016): Radar and LiDAR Sensorfusion in Low Visibility Environments, in Proceedings of the 13th International Conference on Informatics in Control, Automation and Robotics. 13th International Conference on Informatics in Control, Automation and Robotics, Lisbon, Portugal: SCITEPRESS - Science and and Technology Publications, pp. 30–36. Available at: https://doi.org/10.5220/0005960200300036.

Kuhn Christian (2018): Visibility measurements in tunnels – Adjustment of visual range measurent values, Whitepaper, SICK AG, Waldkirch, Deutschland. Available online at https://cdn.sick.com/media/docs/6/06/706/whitepaper_visibility_measurement_in_tunnels_modification_of_the_measuring_results_en_im0082706.pdf

Mielle Malcom; Magnusson Martin; Lilienthal Achim J. (2019): A comparative analysis of radar and lidar sensing for localization and mapping, in 2019 European Conference on Mobile Robots (ECMR). 2019 European Conference on Mobile Robots (ECMR), Prague, Czech Republic: IEEE, pp. 1–6. Available at: https://doi.org/10.1109/ECMR.2019.8870345.

Pfennigbauer Martin; Wolf Clifford; Weinkopf Josef; Ullrich Andreas (2014): Online waveform processing for demanding target situations, in Proc. SPIE 9080-18, Society of Photo-Optical Instrumentation Engineers.

Wallace Andrew; Halimi Abderrahim; Buller Gerald (2020): Full Waveform LiDAR for Adverse Weather Conditions, IEEE transactions on vehicular technology, Vol. 69, No. 7, July 2020.